

Effects of deficiency location on CFRP strengthening of steel CHS short columns

Razieh Shahabi^a and Kambiz Narmashiri^{*}

Department of Civil Engineering, Zahedan Branch, Islamic Azad University, Zahedan, Iran

(Received October 17, 2017, Revised April 13, 2018, Accepted May 23, 2018)

Abstract. Structures may need retrofitting as a result of design and calculation errors, lack of proper implementation, post-construction change in use, damages due to accidental loads, corrosion and changes introduced in new editions of construction codes. Retrofitting helps to compensate weakness and increase the service life. Fiber Reinforced Polymer (FRP) is a modern material for retrofitting steel elements. This study aims to investigate the effect of deficiency location on the axial behavior of compressive elements of Circular Hollow Section (CHS) steel short columns. The deficiencies located vertically or horizontally at the middle or bottom of the element. A total of 43 control column and those with deficiencies were investigated in the ABAQUS software. Only 9 of them tested in the laboratory. The results indicated that the deficiencies had a significant effect on the increase in axial deformation, rupture in deficiency zone (local buckling), and decrease in ductility and bearing capacity. The damages of steel columns were responsible for resistance and stiffness drop at deficiency zone. Horizontal deficiency at the middle and vertical deficiency at the bottom of the steel columns were found to be the most critical. Using Carbon Fiber Reinforced Polymer (CFRP) as the most effective material in retrofitting the damaged columns, significantly helped the increase in resistance and rupture control around the deficiency zone.

Keywords: steel short columns; strengthening; deficiency; CFRP; CHS

1. Introduction

The expired elements of structures are strongly in need of repair and retrofitting. These elements might become weak due to environmental and human factors. In such a case, they need retrofitting. Based on above mentioned issues and high reconstruction costs, a large part of the development budget is annually used to repair and strengthen these structures. Carbon Fiber Reinforced Polymer (CFRP) is a modern material used to help engineers and designers retrofit the structures. These polymers are widely used worldwide to retrofit structures.

Jiao and Zhao (2004) examined the strengthening of butt-welded very high strength (VHS) circular steel tubes retrofitted by CFRP. A total of 21 tubes underwent axial stress test. Three rupture modes (adhesive rupture, CFRP rupture, and combined rupture) were observed. The best epoxy adhesive was selected. Tao *et al.* (2005) investigated the CFRP for strengthening concrete-filled steel tubular columns experimentally. They found out that CFRP was significantly effective in increase in bearing capacity. Increasing number of layers was responsible for the increase in bearing capacity. Teng *et al.* (2005) evaluated the effect of FRP composite strengthening against deformations and rupture modes of steel columns. They found out that FRP campsites under axial loads were

responsible for preventing the early buckling failure and axial deformations of steel columns. The study by Teng and Hu (2007) on the retrofitting thin-walled circular columns using FRP showed that failure in thin-walled steel tubes due to axial load would occur at the outer surface of the column. Strengthening the axial elements by FRP composites was found to be effective for the increase in energy absorption and axial deformation control at the critical zone of steel columns. The fiber is also capable of delaying rupture. The experimental study by Bambach and Elchalakani (2007) on strengthening short box columns using CFRP showed that CFRP was useful for the increase in resistance and energy of the cross sections undergoing compression. The study by Harris *et al.* (2008) on compressed elements in laboratory showed that a little FRP can improve buckling, energy absorption and ultimate ductility. Bambach (2010) showed that the failure energy and short CFRP-squared steel tubes depend on the type of steel and CFRP thickness/width ratio. Using CFRP led to the increase in the ultimate bearing capacity and special energy. The study by Haedir and Zhao (2011) on the design of 10 short CFRP-reinforced steel tubular columns in laboratory showed that using longitudinal and transverse CFRP was responsible for the increase in the yielding capacity. Greater use of CFRP contributed to the delayed buckling. The study by Sivasankar (Sivasankar *et al.* 2012) investigated the failure modes, stress-strain behavior and ultimate bearing capacity of CFRP Jacketed HSS tubular members. Attaching CFRP was found to be an effective method in increasing the bearing capacity and stiffness and delaying buckling. CFRP experienced rupture when the load increased. Kalavagunta

*Corresponding author, Ph.D., Assistant Professor,
E-mail: narmashiri@iauzah.ac.ir

^a M.Sc., E-mail: razishahabi64@gmail.com

et al. (2013) studied the lipped channel steel sections strengthened by CFRP under axial loading. They studied the channel-like column in two methods: the whole column and web in the laboratory. They found out that the bearing capacity increased by 16.75% and 10.26% in the fully strengthened specimen and the specimen strengthened in the web, respectively. Capacity decrease and sudden failure were observed due to the delamination and CFRP separation. Surface preparation and temperature were two important factors to obtain the appropriate adhesion between steel and fiber. Sundarraja and Sivasankar (2013) strengthened 12 CFRP-jacketed HSS tubular members. They considered the number of layers and CFRP strip distance in the laboratory. They concluded that CFRP was responsible for the increase in the bearing capacity. It also delayed the lateral buckling. Using transverse fiber led to greater increase in stiffness, bearing capacity and axial deformation compared to the longitudinal mode. Uriayer and Alam (2013) studied the mechanical properties of steel-CFRP composite specimen under uniaxial tension. Wang and Shao (2014) investigated the compressive performances of concrete filled Square CFRP-Steel Tubes (S-CFRP-CFST). Samaaneh *et al.* (2016) investigated the continuous composite girders strengthened with CFRP. Gholami *et al.* (2016) studied the performance of steel beams strengthened with pultruded CFRP plate under various exposures.

Recently, Ghaemdoust *et al.* (2016) studied CFRP-strengthened SHS short columns. Defects were applied unilaterally and the results were reported based on the structural performance of the columns. They found out that using carbon fiber was responsible for the increase in bearing capacity and delaying of local buckling. Using more layers improved the column performance and compensated the deficiency. Yousefi *et al.* (2017) researched the structural behaviors of notched steel beams upgraded using CFRP strips. Karimian *et al.* (2017) investigated 8 circular steel columns with similar dimensions and cross sections in the laboratory and software. The results showed that deficiency decreased the bearing capacity. The effect of the horizontal defect was greater than the vertical one. Using CFRP for strengthening the circular steel columns with deficiency showed an appropriate effect in increasing the bearing capacity, decreasing stress at defect zone, and preventing local deformations caused by deficiency. In their research, the deficiencies were created just at the middle of the specimens vertically or horizontally.

As it can be seen, few studies were focused on strengthening CHS steel short columns with defects. Most studies have taken squared steel columns into account. This article aimed to investigate the effects of deficiency location

on the behavior of steel short circular columns caused by vertical and horizontal defects under axial loads. CFRP was used for strengthening in order to compensate the bearing capacity loss and prevent the deformations caused by defects. The modeling and laboratory results were investigated.

2. Materials and methods

In this research, 43 specimens with vertical and horizontal defects having different deficiency dimensions and locations were investigated. In the laboratory, only 9 of them tested. In the experimental specimens, a specimen without defects was considered as the control one. Four columns had horizontal defect at the middle and bottom of the columns. Other four columns had vertical defects at the middle and bottom of the columns. Two specimens with horizontal defects and two with vertical defects were strengthened using CFRP. This research focused just on middle and bottom defects.

2.1 Characteristics of selected steel column

Circular Hollow Section (CHS) (Height = 300 mm, Outer Diameter = 165 mm, Thickness = 3 mm, Yielding Stress = 315, Ultimate Stress = 382 MPa, and Ultimate Strain = 19.8%) was taken into account. The columns dimensions and material properties which were obtained by coupon test were tabulated in Table 1. Figs. 1 and 2 show the support and loading conditions, geometric characteristics of columns, and the locations of defects. The height of the columns was chosen as the slenderness ratio of the columns is ranged in the short columns range. In this case, local buckling is taken place as will show in the most

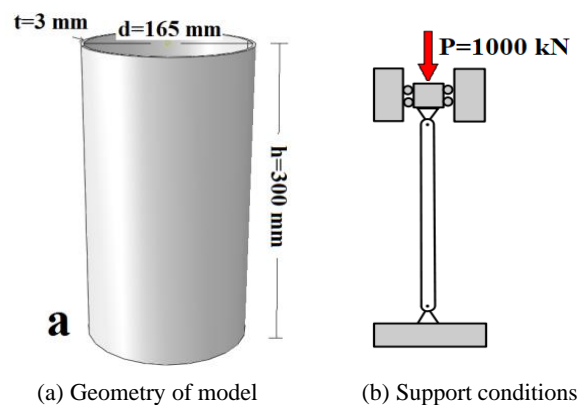


Fig. 1 Schematic of the model

Table 1 Circular steel member dimensions and material property

Metal circular columns specifications						Modulus of elasticity (Gpa)	Stress (Mpa)		Strain (%)
Diameter (mm)	Thickness (mm)	Height (mm)	Cross section (*10 ² mm ²)	Moment of inertia (*10 ⁴ mm ⁴)	Radius of gyration (*10 mm)		Yielding stress (F_y)	Ultimate stress (F_u)	Ultimate stress (ϵ)
165	3	300	213.82	3638.36	4.12	200	315	382	19.8

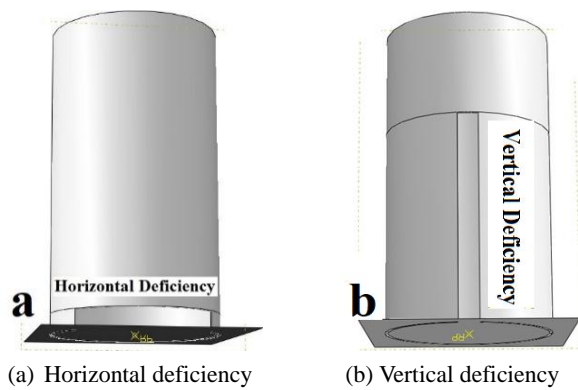


Fig. 2 Deficiency types

experimental figures. The column length is not considered as one of the variables of this research.

2.2 CFRP

In order to strengthen the specimens, CFRP strips (SikaWrap® -230 C) were used. Modulus of Elasticity was 238,000 MPa. Strip thickness and Poisson's ratio were 0.131 mm and 0.12, respectively. The CFRP material property was provided by the manufacturer. Transverse and longitudinal CFRP layers were employed. The first and third layers were transverse, while the second and fourth layers were longitudinal. Stress-Strain diagram shows that they have linear elastic behavior until the rupture without any clear yield point. Table 2 shows the carbon fiber characteristics.

2.3 Adhesive

Adhesive prepares bond between steel surface and composite materials. It also causes the similar function of composite and column. CFRP strips were attached to the steel columns using Sikadur® -330 epoxy with Modulus of Elasticity of 4500 MPa. The adhesive material property was provided by the manufacturer. Table 3 shows the adhesive characteristics.

2.4 Specimens' specifications

A total of 43 steel columns were investigated. The specimens had the same dimensions of steel circular hollow

Table 2 CFRP specifications

Thickness (mm)	Density (* 10 ⁻³ g/mm ³)	Tensile strength (Mpa)	Modulus of elasticity (Mpa)	Ultimate strain (%)
0.131	1.76	4300	238000	1.7

Table 3 Resin epoxy specifications

Tensile strength (Mpa)	Modulus of elasticity (Mpa)	Ultimate strain (%)
0.9	4500	30



Fig. 3 Laboratory specimens before and after sandblasting

section (CHS). One specimen had no deficiency and was chosen as the control one. All other specimens had deficiency with different dimensions, orientations and locations. Some of the specimens had horizontal deficiency and other ones had vertical deficiency. Five of the columns were investigated both experimentally and numerically. All other columns were only simulated numerically. Table 4 shows the steel column characteristics. The specimens' dimensions were measured after cutting and before sandblasting. The reduction of the dimensions due to sandblasting was neglected. All defect lengths were measured for the curvature ones. Acronyms were used to label the specimens as follows: *H* and *V* shows Horizontal and Vertical defects, respectively. *M* and *C* show Middle and Corner defects. *T*, *M* and *B* indicate deficiency location at Top, Middle and Bottom of the columns, respectively. *D* shows that the specimen had deficiency. Four CFRP layers were used for strengthening. Two traverse and two longitudinal layers were employed. Note that Control has no defects. Fig. 3 shows the experimental specimens prior to the test.

2.5 Specimens preparation and experimental test setup

In the experimental study, horizontal and vertical defects were created at the middle and bottom of the steel columns using Computer Numerical Control (CNC) machine. Fig. 4 shows the cutting procedure by CNC. To create clean and corrosion-free specimens, 9 cut steel columns were transferred to the factory. Steel columns were sandblasted in order to attach CFRP sheets. Sandblast degree was chosen 2.5 according to the Swedish Standard (SIS 05 59 00, 1967-Pictorial Surface Preparation Standards for Painting Steel Surfaces). Fig. 5 shows a set of sandblasted steel columns with defects.

To attach CFRP, Sikadur 330 epoxy resin was used with a ratio of 4:1. All strengthened specimens were fully warped by four CFRP layers with 20-mm overlapping. The

Table 4 Specifications, deficiency dimensions, and load bearing capacities of the samples

No	Specimen	Deficiency			CFRP layers	Load bearing capacity				
		Length (mm)	Width (mm)	Position		Experimental		Numerical		Experimental & numerical load difference (%)
						Load (kN)	Inc./ Dec. (%)	Load (kN)	Inc./ Dec. (%)	
1	Control	N/A	N/A	N/A	N/A	380	-	398	-	4.70
2	MTHD-65-5	65	5	Top-Horizontal	N/A	N/A	N/A	356	-10.55	N/A
3	MTHD-65-10	65	10	Top-Horizontal	N/A	N/A	N/A	352	-11.55	N/A
4	MTHD-65-20	65	20	Top-Horizontal	N/A	N/A	N/A	347	-12.81	N/A
5	MTHD-129-5	129	5	Top-Horizontal	N/A	N/A	N/A	332	-16.58	N/A
6	MTHD-129-10	129	10	Top-Horizontal	N/A	N/A	N/A	327	-17.83	N/A
7	MTHD-129-20	129	20	Top-Horizontal	N/A	N/A	N/A	323	-18.84	N/A
8	MTHD-129-20-4CFRP	129	20	Top-Horizontal	4	N/A	N/A	384	-3.51	N/A
9	MHD-65-5	65	5	Middle-Horizontal	N/A	N/A	N/A	340	-14.57	N/A
10	MHD-65-10	65	10	Middle-Horizontal	N/A	N/A	N/A	339	-14.82	N/A
11	MHD-65-20	65	20	Middle-Horizontal	N/A	N/A	N/A	336	-15.57	N/A
12	MHD-129-5	129	5	Middle-Horizontal	N/A	N/A	N/A	321	-19.34	N/A
13	MHD-129-10	129	10	Middle-Horizontal	N/A	N/A	N/A	320	-19.59	N/A
14	MHD-129-20	129	20	Middle-Horizontal	N/A	292	-23.15	317	-20.35	8.56
15	MHD-129-20-4CFRP	129	20	Middle-Horizontal	4	370	-2.63	397	-0.25	7.29
16	MHBD-65-5	65	5	Bottom-Horizontal	N/A	N/A	N/A	356	-10.55	N/A
17	MHBD-65-10	65	10	Bottom-Horizontal	N/A	N/A	N/A	352	-11.55	N/A
18	MHBD-65-20	65	20	Bottom-Horizontal	N/A	N/A	N/A	345	-13.31	N/A
19	MHBD-129-5	129	5	Bottom-Horizontal	N/A	N/A	N/A	355	-10.80	N/A
20	MHBD-129-10	129	10	Bottom-Horizontal	N/A	N/A	N/A	355	-10.80	N/A
21	MHBD-129-20	129	20	Bottom-Horizontal	N/A	303	-20.26	327	-17.83	7.90
22	MHBD-129-20-4CFRP	129	20	Bottom-Horizontal	4	381	-0.26	366	-8.04	3.93
23	MTVD-150-5	150	5	Top-Vertical	N/A	N/A	N/A	346	-13.06	N/A
24	MTVD-150-10	150	10	Top-Vertical	N/A	N/A	N/A	343	-13.81	N/A
25	MTVD-150-20	150	20	Top-Vertical	N/A	N/A	N/A	337	-15.32	N/A
26	MTVD-200-5	200	5	Top-Vertical	N/A	N/A	N/A	345	-13.31	N/A
27	MTVD-200-10	200	10	Top-Vertical	N/A	N/A	N/A	342	-14.07	N/A
28	MTVD-200-20	200	20	Top-Vertical	N/A	N/A	N/A	335	-15.82	N/A
29	MTVD-200-20-4CFRP	200	20	Top-Vertical	4	N/A	N/A	399	0.25	N/A
30	MVD-150-5	150	5	Middle-Vertical	N/A	N/A	N/A	338	-15.07	N/A
31	MVD-150-10	150	10	Middle-Vertical	N/A	N/A	N/A	333	-16.33	N/A
32	MVD-150-20	150	20	Middle-Vertical	N/A	N/A	N/A	326	-18.09	N/A
33	MVD-200-5	200	5	Middle-Vertical	N/A	N/A	N/A	334	-16.08	N/A
34	MVD-200-10	200	10	Middle-Vertical	N/A	N/A	N/A	331	-16.83	N/A
35	MVD-200-20	200	20	Middle-Vertical	N/A	324	-14.73	313	-21.35	3.39
36	MVD-200-20-4CFRP	200	20	Middle-Vertical	4	460	21.05	468	17.58	1.73
37	MVBD-150-5	150	5	Bottom-Vertical	N/A	N/A	N/A	335	-15.82	N/A
38	MVBD-150-10	150	10	Bottom-Vertical	N/A	N/A	N/A	331	-16.83	N/A
39	MVBD-150-20	150	20	Bottom-Vertical	N/A	N/A	N/A	325	-18.34	N/A
40	MVBD-200-5	200	5	Bottom-Vertical	N/A	N/A	N/A	333	-16.33	N/A
41	MVBD-200-10	200	10	Bottom-Vertical	N/A	N/A	N/A	330	-17.08	N/A
42	MVBD-200-20	200	20	Bottom-Vertical	N/A	330	-13.15	323	-18.84	2.50
43	MVBD-200-20-4CFRP	200	20	Bottom-Vertical	4	466	+22.63	490	+23.11	5.15

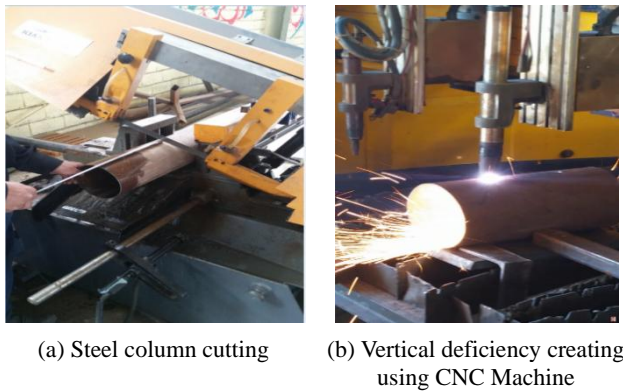


Fig. 4 Experimental specimens preparation

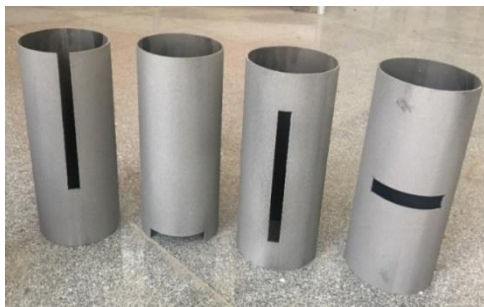


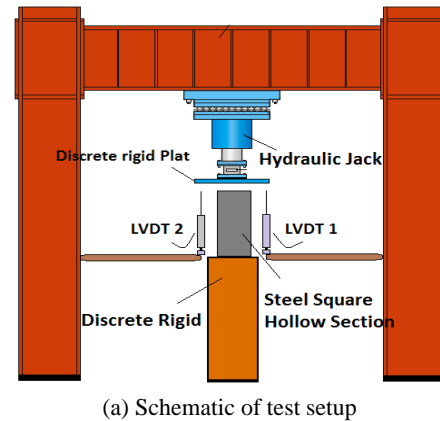
Fig. 5 Sandblasted specimens

specimens were strengthened by two transverse and two longitudinal layers. The first and third CFRP layers were wrapped in the transverse direction, and the second and fourth layers were wrapped in the longitudinal direction. The starting point of the CFRP layer wrapping was not located at the deficiency area. The effects of number of CFRP layers and wrapping area are not investigated in this study.

In order to study the effect of deficiency location on bearing capacity of CHS short steel columns, the specimens were placed on the base with the consideration of hydraulic jack axis. The force was axially applied. Displacement was measured by two LVDTs. Fig. 6 shows the compression test in the laboratory. LOADCELL and LVDT were connected to the DATA LOGGER in order to record and save the data. The load was gradually imposed by the jack. The test method was load-control type, and the minimum loading rate was used. When the ultimate load was decreased suddenly by 20%, then the loading was stopped automatically due to safety. Afterward, the manual loading method can be used. Finally, the bearing capacity and deformation were accurately saved.

2.6 Modeling

ABAQUS software Ver. 6.13 was employed for modeling the specimens. Since 3D analysis and simulation using Solid elements can validate modelling appropriately (Narmashiri and Zamin Jumaat 2011), then in this research abovementioned analysis method and element type are used. The steel columns, CFRP sheets and adhesive were



(a) Schematic of test setup



(b) Experimental test setup

Fig. 6 Test setup

modelled in 3D case. SOLID elements were C3D20R, indicating a 20-node 3D element by reduced integration. Tie was used to attach the CFRP to adhesive and steel columns. Linear and isotropic properties were taken into account for CFRP. Non-linear properties were used for steel modeling. Static general method was used for the analysis. Load was axially imposed on the column. In order to reach the failure mode and detect the post buckling, Riks analysis was used. Usually, Riks method is used to guess unstable, geometrically nonlinear break fall of a structure, which includes nonlinear materials and boundary conditions. Also, it uses the load extent as a surplus unknown; it solves concurrently for loads and displacements. Hence, another quantity must be used to measure the progress of the solution; Abaqus/Standard employs the arc length, along the static equilibrium path in load-displacement space. In this research, software default values were utilized which consists of arc length growth and total arc length amount. The selected element 3D 20-node element has a reduced integration. Tie Method was employed to connect the adhesive and CFRP to the steel column and to generate the desire surface interaction. Linear and isotropic properties were taken into account (Karimian *et al.* 2017). Laboratory specimens used by Haedir and Zhao (2011) were employed for calibration. They used circular steel elements (Diameter = 43.6 mm, Height = 275 mm, Thickness = 3 mm, Modulus of Elasticity = 200 GPa, Poisson's ratio = 0.3, and Ultimate Resistance = 507 GPa). Mesh sizes of 9, 10, and 11 mm

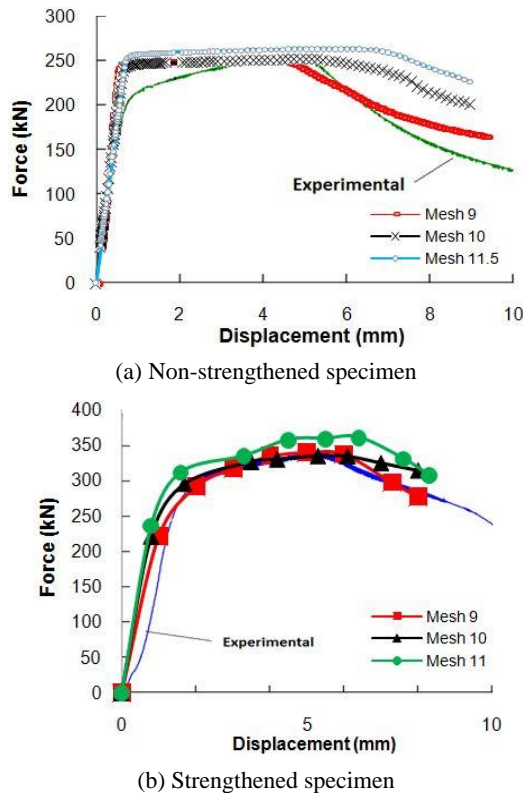


Fig. 7 Force-displacement validation using different meshing sizes

were used for modeling both strengthened and non-strengthened specimens investigated by Haedir and Zhao (2011). Fig. 7 indicates axial load-axial deformation of their specimens. According to Fig. 7(a), the bearing capacity difference percentage for non-strengthened specimen is seen 8% in 11-mm for non-strengthened specimen compared to 9-mm mesh. 10 mm-mesh had similar capacity to 9-mm one. In terms of fail time, 9-mm mesh showed better compatibility. The compatibility of 9-mm mesh modeling with laboratory specimen for both strengthened (Fig. 7(b)) and non-strengthened specimens (Fig. 7(a)) shows the correct selection of mesh, optimal boundary conditions, and appropriate software modeling.

3. Results and discussions

The results of control specimen were considered the basis of comparison. The comparisons were based on bearing capacity and deformations. The article aimed to analyze the effect of location of defects, and CFRP strengthening. According to Table 4, it is shown that for all deficient specimens, by increasing the dimensions of the deficiency, the bearing capacity of the columns reduced.

3.1 Horizontal defect at the middle of column

As it can be seen in Fig. 8(b), the deformation caused by compression loading of steel columns with horizontal defect caused the rupture and decrease in defect width at the middle of the element. This was responsible for the decrease in resistance and stiffness. Table 4 shows that the defect was responsible for the decrease in bearing capacity by almost 23.15% compared to the control. As it is evident in Fig. 8(c), strengthening by four CFRP layers in the steel column with horizontal defect increased the stiffness and delayed rupture in the walls. This was responsible for the increase in resistance and bearing capacity by up to 370 KN. Note that the initial failure of carbon fiber was observed at 200 KN in steel columns strengthened by four CFRP layers. Loading time increased contributed to greater failure percentage and rupture at CFRP zone.

3.2 Horizontal defect at the bottom of column

According to Fig. 9(b), horizontal defect at the bottom of the steel column (MHBD-129-20) increased deformation around the defect and, accordingly, rupture and accretion. This was responsible for the decrease in bearing capacity by almost 20.26% compared to control. Note that the defect was not effective in buckling. Strengthening coupled with the significant decrease in compressive stress at the defect zone improved the performance and increased the bearing capacity by 381 KN (Fig. 9(c)).

3.3 Vertical defect at the middle of column

Fig. 10(b) shows the vertical defect at the middle of the column. The resistance decrease in bearing capacity was

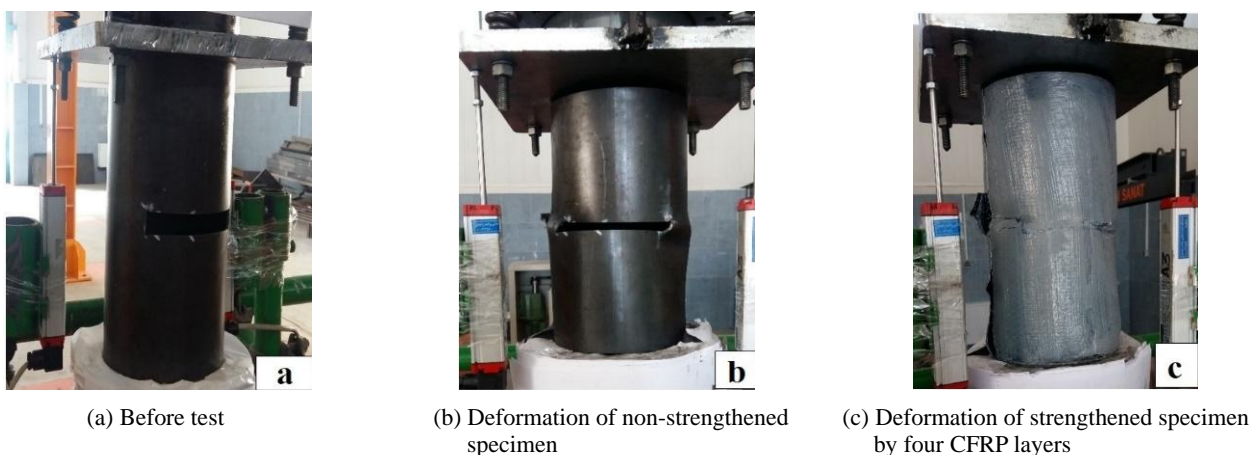


Fig. 8 Column with horizontal deficiency at the middle of column

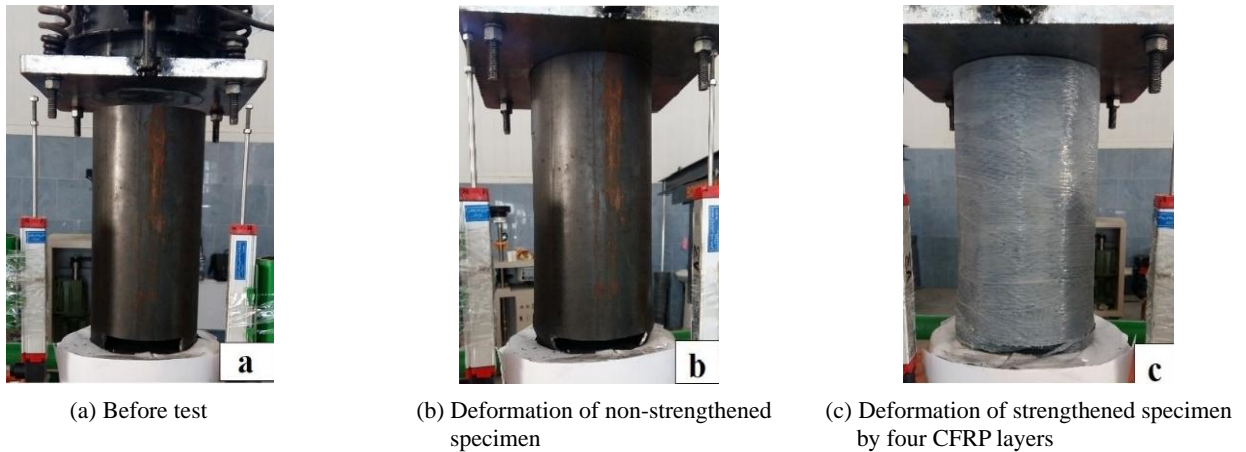


Fig. 9 Column with horizontal deficiency at the bottom of column

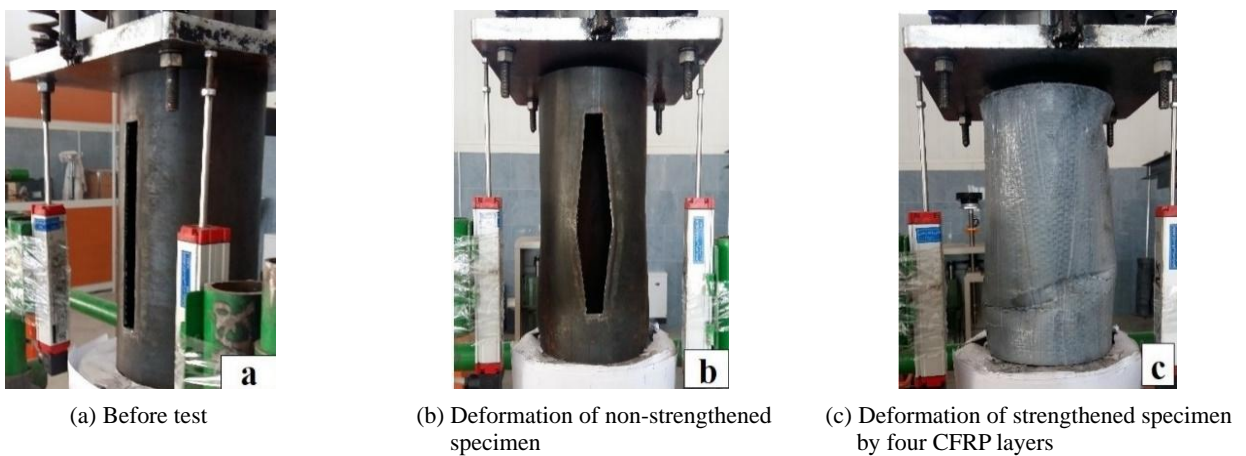


Fig. 10 Column with vertical deficiency at the middle of column

responsible for the increase in defect length and Von-Mises intensification including compressive and shear stress at defect edges and tensile stress at the middle of the defect. Bearing capacity decrease was reported by 14.73% compared to the control. Using CFRP increased the bearing capacity by up to 460 kN. Such resistance increase met the shortcoming. Fig. 10(c) shows the deformation of the

strengthened column with vertical defect.

3.4 Vertical defect at the bottom of column

According to Fig. 10(b), it is clear that the vertical defect at the bottom of the column caused local buckling and defect width opening. Note that, according to Table 4,

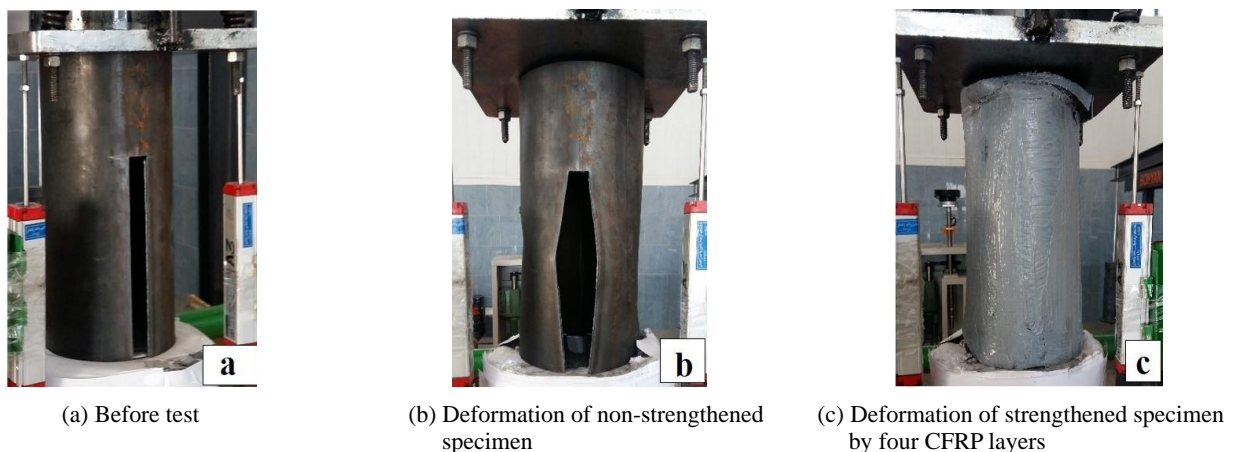


Fig. 11 Column with vertical deficiency at the bottom of column



Fig. 12 Ultimate deformation of control (specimen without defect)

the decrease in bearing capacity as a result of vertical defect decreased by almost 13.15% compared to the control. Fig. 11(c) shows that carbon layers covered and strengthened the element undergoing compressive loading, which was responsible for the increase in stiffness. Using four layers of CFRP contributed to the increase in the bearing capacity of the column with vertical defect by up to 466 kN.

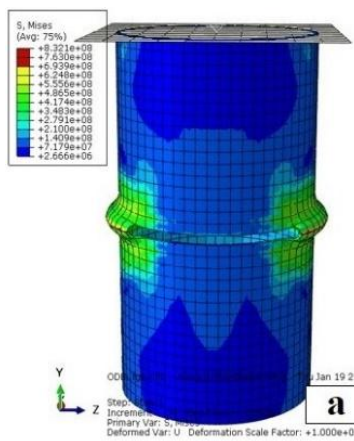
3.5 Failure modes of CHS columns

3.5.1 Failure mode of control

According to Fig. 12, the control specimen was tested until the completed rupture. The outer walls of the columns experienced Elephant-Foot Buckling as a result of compressive loading at the end zone. Laboratory results showed that the initial deformation began from 200 kN load. As loading time increased, bearing capacity continued to the maximum level. The increase in loading caused local buckling at the outer walls of the steel column. Fig. 12 shows the deformations and axial rupture of the control.

3.5.2 Failure modes of columns with horizontal defects

Fig. 13 shows the horizontal defect at the middle of the CHS columns. After completed axial loading, it was found that the horizontal defect at the middle caused great deformation, reduced stiffness, and increased local buckling at the middle walls. Rupture began at almost 144 kN. Axial deformation continued until 292 kN. As it is evident, after finishing loading, the defect width decreased and accretion was observed at the defect zone. Fig. 14 shows the

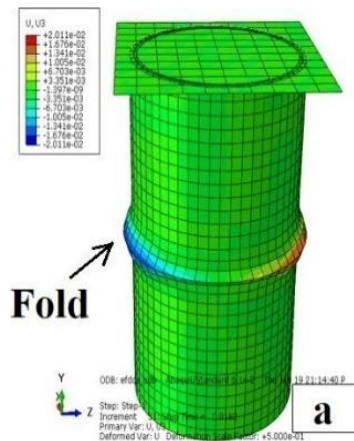


(a) Von-Mises Stress (modelling)



(b) Experimental test

Fig. 13 Ultimate deformation of non-strengthened steel column having horizontal deficiency at the middle of column

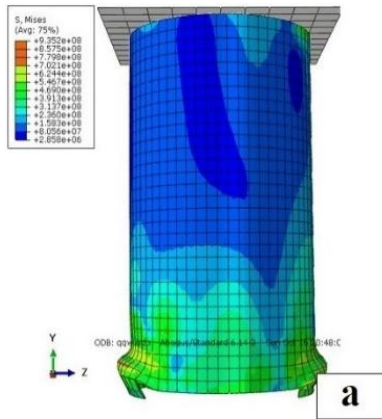


(a) Von-Mises Stress (modelling)



(b) Experimental test

Fig. 14 Ultimate deformation of strengthened steel column having horizontal deficiency at the middle of column

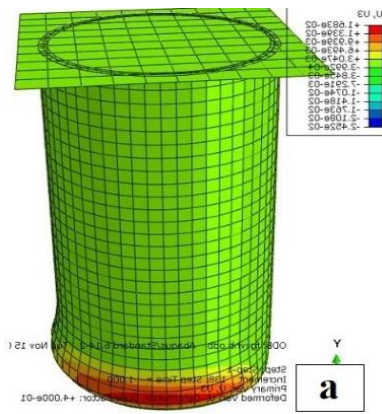


(a) Von-Mises Stress (modelling)



(b) Experimental test

Fig. 15 Ultimate deformation of non-strengthened steel column having horizontal deficiency at the bottom of column



(a) Von-Mises Stress (modelling)

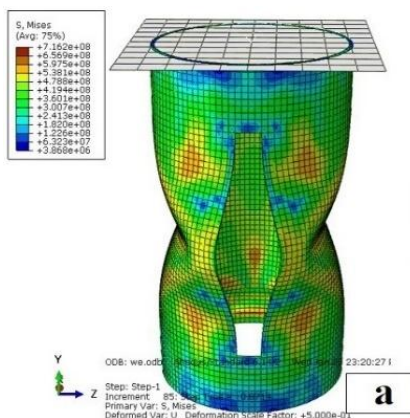


(b) Experimental test

Fig. 16 Ultimate deformation of strengthened steel column having horizontal deficiency at the bottom of column

strengthened column with horizontal defect using four CFRP layers. Strengthening horizontal defect increased the resistance. The failure and fiber separation occurred at the defect zone at the middle of the compressive element. The horizontal defect at the bottom of the steel column caused axial deformation compared to the control. As it is evident

in Fig. 15, the increase in length caused increased yielding at the support zone. This damage at the end of the steel column increased the compression at support zone under axial loading. Using carbon fiber for strengthening the columns with horizontal defect showed that the defect was capable of improving the performance (Fig. 16).

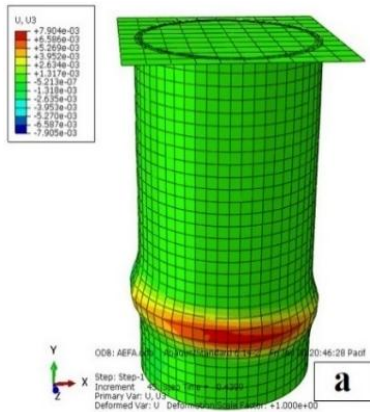


(a) Von-Mises Stress (modelling)



(b) Experimental test

Fig. 17 Ultimate deformation of non-strengthened steel column having vertical deficiency at the middle of column



(a) Von-Mises Stress (modelling)



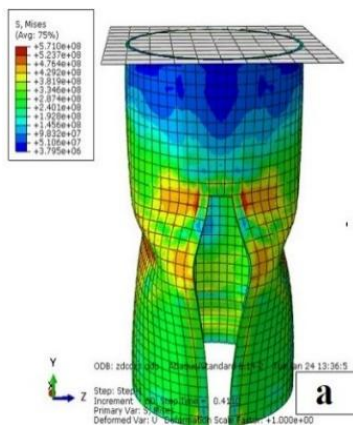
(b) Experimental test

Fig. 18 Ultimate deformation of strengthened steel column having vertical deficiency at the middle of column

3.5.3 Failure mode of specimens with vertical defect

Fig. 17 shows the vertical defects at the middle of the CHS columns. Axial loading showed that the vertical defect in the middle of the column opened the defect width. It was also responsible for the decrease in stiffness and increase in

local buckling in middle walls. The rupture began at almost 198 kN. Axial deformations continued up to 324 kN. Fig. 18 shows the strengthening of columns with vertical defects using four CFRP layers. Vertical defect strengthening increased the resistance and controlled the local buckling. Carbon fiber rupture happened at the defect zone at the

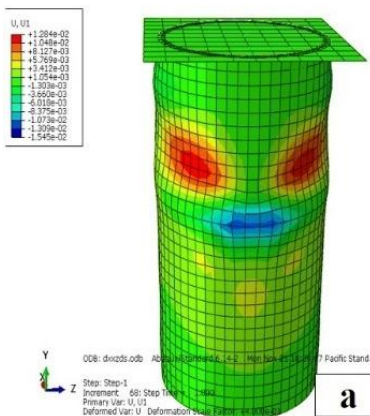


(a) Von-Mises Stress (modelling)



(b) Experimental test

Fig. 19 Ultimate deformation of non-strengthened steel column having vertical deficiency at the bottom of column



(a) Von-Mises Stress (modelling)



(b) Experimental test

Fig. 20 Ultimate deformation of strengthened steel column having vertical deficiency at the bottom of column

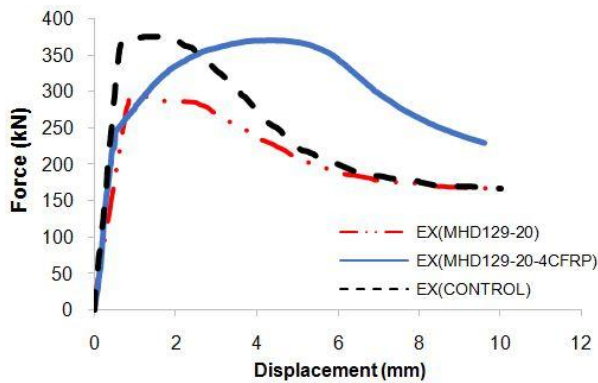


Fig. 21 Force-displacement graph for columns having horizontal defect at the middle

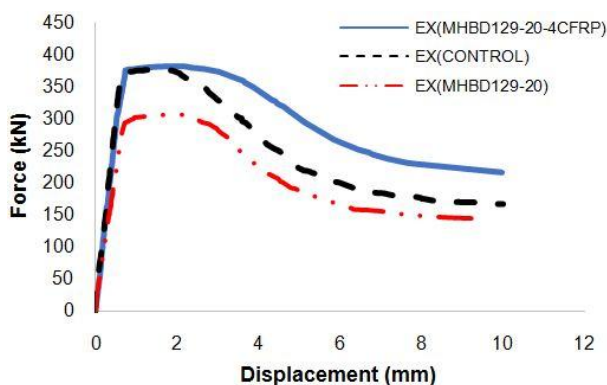


Fig. 22 Force-displacement graph for columns having horizontal defect at the bottom

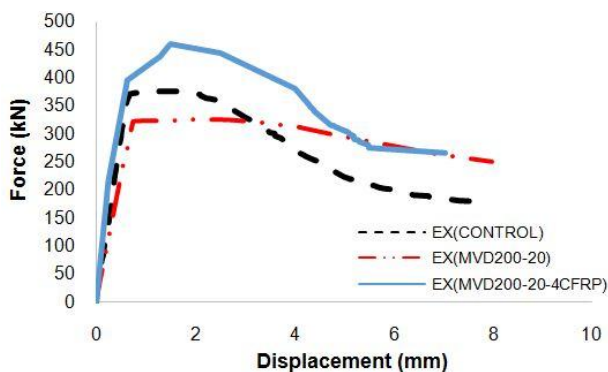


Fig. 23 Force-displacement graph for columns having vertical defect at the middle

longitudinal range.

Fig. 19 shows the vertical defect at the bottom of the column (MVBD-200-20). Axial loading on the columns with defect was associated with significant stiffness decrease compared to control. Horizontal defect had greater effect in resistance decrease and ultimate deformation compared to the vertical defect. CFRP composites played a key role in improving compressive element so that it increased the stiffness and resistance. Using CFRP was very effective in controlling elephant foot buckling. Fig. 20 shows the effect of CFRP.

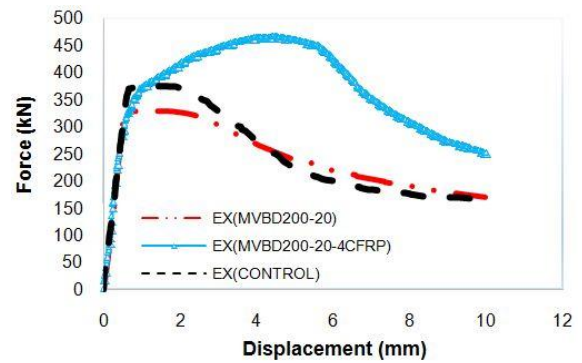


Fig. 24 Force-displacement graph for columns having vertical defect at the bottom

3.6 Bearing capacity of columns

As it can be seen from Figs. 21 to 24, the columns with defects were compared with the control. The comparison of force-displacement of columns with defect showed that the defect columns experienced resistance drop and significantly reduced bearing capacity compared to control. The effect of using CFRP for improving the performance of columns showed that carbon fiber coverage at outer surface increased the stiffness and performance in line with the increase in bearing capacity. Using CFRP helped significantly to delay the local buckling of compressive element.

4. Conclusions

The results of this study showed that location of defects were effective in reducing value of bearing capacity of steel CHS short columns. Increasing the dimensions of deficiency caused more reduction in bearing capacity of the columns. Carbon fiber as an efficient material was effective in bearing capacity of damaged element strengthening. A total of 43 specimens were investigated numerically and only 9 specimens were studied experimentally. The results were compared with ABAQUS. Good correlation was found between test and modeling results. The defect increased deformation and rupture at compressive loading. Increasing longitudinal and transverse dimensions showed that resistance drop was experienced as a result of compressive loading. At the same time, axial deformations increased. The horizontal defects in the middle of the columns had the greatest decrease in bearing capacity. The defect in the middle of the steel columns decreased the bearing capacity by almost 23.15% compared to the control. The bearing capacity decrease was compensated by four CFRPO layers. The vertical defect in the middle of the steel column decreased the bearing capacity by 14.73% compared to the control. For the vertical defect at the bottom of the columns, resistance drop was experienced by almost 13.15% compared to control. Increasing loading was responsible for the increase in stress at defect zone and gradual local buckling. Increasing loading accelerated the failure after passing elastic zone. Using four CFRP layers not only compensated the bearing capacity decrease but also were

effective in reducing and delaying local buckling. It controlled the buckling very well. Covering outer surface of steel columns with defects using carbon fiber increased the stiffness, controlled the rupture, and caused optimal performance in line with bearing capacity increase. Carbon fiber was very effective in increasing resistance and ductility and delaying local buckling of compressive elements.

Acknowledgments

Islamic Azad University, Zahedan Branch, Zahedan, Iran, and Iranian Construction Engineering Organization, Sistan and Baluchestan Province, Zahedan, Iran financially supported the study presented here. Authors would like to record their appreciations for the supports.

References

- Bambach, M.R. (2010), "Axial capacity and crushing behavior of metal-fiber square tubes – Steel, stainless steel and aluminum with CFRP", *Compos. Part B: Eng.*, **41**(7), 550-559.
- Bambach, M. and Elchalakani, M. (2007), "Plastic mechanism analysis of steel SHS strengthened with CFRP under large axial deformation", *Thin-Wall. Struct.*, **45**(2), 159-170.
- Ghaemdoost, M.R., Narmashiri, K. and Yousefi, O. (2016), "Structural behaviors of deficient steel SHS short columns strengthened using CFRP", *Constr. Build. Mater.*, **126**, 1002-1011.
- Gholami, M., Mohd Sam, A.R., Marsono, A.K., Tahir, M.M. and Faridmehr, I. (2016), "Performance of steel beams strengthened with pultruded CFRP plate under various exposures", *Steel Compos. Struct., Int. J.*, **20**(5), 999-1022.
- Haedir, J. and Zhao, X.L. (2011), "Design of short CFRP-reinforced steel tubular columns", *J. Constr. Steel Res.*, **67**(3), 497-509.
- Harries, K.A., Peck, A. and Abraham, E.J. (2008), "FRP-Stabilised Steel Compression Members", *Proceedings of the 4th International Conference on FRP Composites in Civil Engineering*, Zurich, Switzerland, July.
- Jiao, H. and Zhao, X.L. (2004), "CFRP strengthened butt-welded very high strength (VHS) circular steel tubes", *Thin-Wall. Struct.*, **42**(7), 963-978.
- Kalavagunta, S., Naganathan, S. and Bin Mustapha, K.N. (2013), "Proposal for design rules of axially loaded CFRP strengthened cold formed lipped channel steel sections", *Thin-Wall. Struct.*, **72**, 14-19.
- Karimian, M., Narmashiri, K., Shahraki, M. and Yousefi, O. (2017), "Structural behaviors of deficient steel CHS short columns strengthened using CFRP", *J. Constr. Steel Res.*, **138**, 555-564.
- Narmashiri, K. and Zamin Jumaat, M. (2011), "Reinforced steel I-beams: A comparison between 2D and 3D simulation", *Simul. Model. Pract. Theory*, **19**(1), 564-585.
- Samaaneh, M.A., Sharif, A.M., Baluch, M.H. and Azad, A.K. (2016), "Numerical investigation of continuous composite girders strengthened with CFRP", *Steel Compos. Struct., Int. J.*, **21**(6), 1307-1325.
- Sivasankar, S., Thilakranjith, T. and Sundarraja, M.C. (2012), "Axial Behavior of CFRP Jacketed HSS Tubular Members- An Experimental Investigation", *Int. J. Earth Sci. Eng.*, 1729-1737.
- Sundarraja, M.C. and Sivasankar, S. (2013), "Behaviour of CFRP jacketed HSS tubular members under compression an experimental investigation", *J. Struct. Eng.*, **39**(S), 574-582.
- Swedish Standard SIS 05 59 00 (1967), Pictorial Surface Preparation Standards for Painting Steel Surfaces.
- Tao, Z., Han, L. and Zhuang, J.P. (2005), "Using CFRP to strengthen concrete-filled steel tubular columns: sub column tests", *Proceedings of the 4th International Conference on Advances in Steel Structures*, Shanghai, China, June, pp. 701-706.
- Teng, J.G. and Hu, Y.M. (2007), "Behaviour of FRP-jacketed circular steel tubes and cylindrical shells under axial compression", *Constr. Build. Mater.*, **21**(4), 827-838.
- Teng, J.G., Chen, J.F., Smith, S.T. and Lam, L. (2005), *FRP-Strengthened RC Structures*, Wiley.
- Uriayer, F.A. and Alam, M. (2013), "Mechanical properties of steel-CFRP composite specimen under uniaxial tension", *Steel Compos. Struct., Int. J.*, **15**(6), 659-677.
- Wang, Q. and Shao, Y. (2014), "Compressive performances of concrete filled Square CFRP-Steel Tubes (S-CFRP-CFST)", *Steel Compos. Struct., Int. J.*, **16**(5), 455-480.
- Yousefi, O., Narmashiri, K. and Ghaemdoost, M.R. (2017), "Structural behaviors of notched steel beams strengthened using CFRP strips", *Steel Compos. Struct., Int. J.*, **25**(1), 35-43.

DL